ELSEVIER

Journal of Photochemistry and Photobiology A: Chemistry 149 (2002) 237–245

Journal of Photochemistry and Photobiology A:Chemistry

www.elsevier.com/locate/jphotochem

Short communication

Preparation, characterization and photocatalytic activity of nanocrystalline thin film TiO_2 catalysts towards 3,5-dichlorophenol degradation

I.M. Arabatzis [a,b], S. Antonaraki [a,b], T. Stergiopoulos [a], A. Hiskia [a], E. Papaconstantinou [a], M.C. Bernard [c], P. Falaras [a,*]

[a] *Institute of Physical Chemistry, NCSR "Demokritos", 153 10 Aghia Paraskevi Attikis, Greece*
[b] *Department of Chemical Engineering, National Technical University of Athens, Iroon Polytechniou 9, 157 80 Zografou, Athens, Greece*
[c] *UPR 15, CNRS, UPMC, 4 Place Jussieu, 75252 Paris Cedex 05, France*

Received 5 November 2001; received in revised form 21 November 2001; accepted 26 November 2001

Abstract

Both opaque and transparent TiO_2 nanocrystalline thin films were developed on glass substrates by applying dip coating and doctor-blade deposition techniques, using titanium(IV) butoxide and Degussa P25 TiO_2 powder as precursor and starting material, respectively. Atomic force microscopy (AFM) and scanning electron microscopy (SEM) evaluated the surface characteristics of the films. Results on their structure and crystallinity were obtained by means of X-ray diffraction and Raman spectroscopy. The catalytic activity of the films towards photodegradation of 3,5-dichlorophenol (3,5-DCP) pollutant was examined and their efficiency was compared to that of the TiO_2 powder (slurry) suspensions. Pseudo-first-order photodegradation kinetics were observed and the reaction constants were determined. It has been shown that the film photocatalysts can efficiently decompose the pollutant, although relatively higher decomposition rates were observed with the commercial starting powder. Differences in the film efficiencies can be attributed to differences in their grain size, surface roughness and fractal parameters. No altering on the doctor-blade films surface characteristics was observed for several hours of cyclic operation during which their photocatalytic efficiency remained remarkably stable.

Keywords: Surface properties; TiO_2 films; Dip coating; Doctor blade; 3,5-Dichlorophenol; Photocatalysis

1. Introduction

There is today a growing interest in developing new and efficient cleaning technologies for environmental protection and remediation. Various toxic and hazardous organic compounds present in wastewater and surface water are difficult to be decomposed by conventional chemicals (ozone, chlorine, hydrogen peroxide, etc.) or biological methods, especially if they are present at low concentrations. Thus, it has been necessary to develop more effective processes for the degradation of such pollutants. Advanced oxidation processes (AOP) are very promising oxidative mineralization methods. These methods are based mainly on the formation of very reactive and oxidizing free radicals that are able to decompose numerous organic pollutants to CO_2, H_2O and inorganic salts [1,2]. They involve mainly ^{60}Co-γ-radiation, UV light, UV light in the presence of ozone and/or hydrogen peroxide, UV and near-visible light in the presence of titanium dioxide or polyoxometalates.

Titanium dioxide is a non-toxic material. TiO_2 thin films exhibit high stability in aqueous solutions, no photocorrosion under band gap illumination and exceptional surface properties. Their electrochromic behavior is well established [3] but TiO_2 is no longer used in electrochromic devices because its coloration efficiency η is too low. On the contrary, TiO_2 thin films are already widely used in dye-sensitized solar cells [4–6], and lithium insertion batteries [7]. Titanium dioxide appears to be one of the most important photocatalytic materials in the area of environmental purification and especially in heterogeneous photocatalysis, an attractive low temperature, low cost, non-energy consuming technique, where a catalyst is capable of entirely decomposing organic pollutants in both the liquid [8–10] and gaseous phase [11,12] by using solar light illumination. The material in the form of powder suspensions has extensively been used for water treatment involving a large number of organic substrates [13–15].

* Corresponding author. Tel.: +30-1-6503644; fax: +30-1-6511766.
E-mail address: papi@mail.demokritos.gr (P. Falaras).

1010-6030/02/$ – see front matter
PII: S1010-6030(01)00645-1

The basic photocatalytic principle relies on the UV or near-visible photogenerated electrons (e^-) and holes (h^+), which both can contribute to the organic substrate degradation [9,16]. The holes (h^+) and the $^\bullet$OH radicals formed by the reaction with hydroxide anions or water are the major oxidative species for decomposition of organic pollutants. However, several practical problems arising from the use of powder are obvious during the photocatalytic process [12]: (a) separation of the insoluble catalyst from the suspension is difficult, (b) the suspended particles tend to aggregate especially at high concentrations and (c) suspensions are difficult to apply to continuous flow systems.

The immobilization of the photocatalyst in the form of a thin film not only provides an advantage over the drawbacks encountered with powder suspensions but could also endow the surface with photoinduced hydrophilicity [9]. Thus, very recently, TiO_2 thin films have been successfully used for the photocatalytic degradation of 2,4-dichlorophenol [17]. Chlorophenols are used in the pesticide field as disinfectants, fungicides and are also important chemicals or byproducts in a number of industrial processes and are considered by the US Environmental Protection Agency as top priority pollutants [18]. They are persistent compounds under environmental conditions and present high toxicity due to their chlorine substituents. The 3,5-dichlorophenol (3,5-DCP) isomer has a high degradation rate comparing to other isomers and for that reason it has been used for the evaluation of the photocatalytic activity of the nanocrystalline TiO_2 films. The final goal of the study is to develop a general procedure for complete mineralization of this class of toxic and hazardous organic compounds to carbon dioxide by a simple dip-and-pull process with no additional separation step.

2. Experimental

2.1. Materials

3,5-DCP and all reagents, utilized for the synthesis of TiO_2 thin film catalysts were of analytical grade from Fluka AG (Switzerland). Acetonitrile was gradient grade from Merck (Darmstadt, Germany). Syringe driven unit with PVDF Durapore filter (0.45 μm Millex) from Millipore (Bedford, USA) was used for the filtration of TiO_2 slurry. Ultra-pure water was obtained from an USF Purelab plus (Germany) apparatus.

2.2. Preparation of the TiO_2 films

2.2.1. Preparation of the TiO_2 films using the doctor-blade technique

Opaque TiO_2 thin nanostructured films were deposited on optically transparent microscopy glass substrates, ultrasonically cleaned in ethanol prior to use. The method follows, with some modifications, the procedure described in Refs. [19–21]. Grinding 0.5 g TiO_2 powder (Degussa P25) with 1 ml of water containing 0.1 ml acetylacetone produces a viscous paste. The paste is diluted by very slow addition of 1.7 ml of water. Finally, 1 drop of Triton X-100 was added and the paste is smeared on a glass substrate immobilized by an adhesive tape strip, which determines the film thickness. After drying at 100 °C for about 10 min, the film is annealed in an oven at 450 °C for 30 min.

2.2.2. Preparation of the TiO_2 films using the sol–gel process

The general procedure applied is described in Ref. [22]. The 1.72 g titanium butoxide was added dropwise to a solution of 2.5 M pentane-2,4-dione (acetylacetone) in *n*-butanol. The overall volume after addition was 100 ml. The mixture was stirred at room temperature for 15 min yielding, exothermally, a yellow solution. During stirring time, 1 ml aqueous solution of 0.19 g *p*-toluene sulfonic acid was prepared and added to the butanol–titanium complex solution. This was followed by an overnight heating at 60 °C. The resulting orange-yellow sols were stable for several months. TiO_2 thin nanostructured films were deposited on optically transparent microscopy glass substrates, ultrasonically cleaned in ethanol prior to use. The substrates were dip-coated with a constant withdraw speed of 2cm/min 13 cycles of film deposition were applied: each cycle involves dipping to the resulting sol, heating of the film at 100 °C for 15 min and annealing in an oven at 450 °C for 30 min.

2.3. Characterization of TiO_2 films

The film crystallinity was analyzed with X-ray diffraction (Siemens D-500, Cu Kα radiation) and by Raman spectroscopy (DILOR OMARS 89 spectrometer equipped with a CCD detection and using an Argon laser line at 514.5 nm). Detailed surface images were obtained by means of a scanning electron microscope with numerical image acquisition (LEICA S440). Surface morphology, roughness and fractality of the films were also determined with a Digital Instruments Nanoscope III atomic force microscope (AFM), operating in the tapping mode (TM). For the fractal analysis the V423r3 algorithm was used. The algorithm divides the three-dimensional film surface into a series of triangles. The size L of triangles is varied and the surface area of each triangle is calculated and recorded for each size L. The logarithmic plot of the cell size versus the surface area determines the fractal value of the surface (the fractal dimension D_f is defined as the slope of the line obtained by plotting the log of the cell size versus the log of the cell surface area).

2.4. Photocatalytic degradation

The photocatalytic activity of the TiO_2 films deposited on microscopy glass substrates was evaluated by degradation of 3,5-DCP. Photocatalysis experiments were carried out in round-bottomed photocatalytic cells. The Pyrex glass

cell is transparent to radiation over 300 nm. A laboratory constructed "solarbox" equipped with four F15W/T8 black-light tubes (Sylvania GTE) provided the UV–Vis irradiation source. This UV–Vis source has a maximum emission at 375 nm and emits 71.7 $\mu W\,cm^{-2}$ at a distance of 25 cm. The 4 ml of aqueous solution 3,5-DCP 10^{-3} M in the presence of TiO_2 thin films were photolyzed under magnetic stirring. The TiO_2 films were adjusted accurately in surface area at 0.8 cm^2, by cutting the microscope glass slides with a diamond knife. For comparison, the pollutant solution (4 ml) was also photolyzed in the presence of a slurry suspension of Degussa P25 powder (1625 ppm) under the same conditions.

2.5. Analytical determination of 3,5-DCP

3,5-DCP analysis was carried out using an HPLC apparatus consisted of a Waters (Milford, MA) Model 600E pump associated with a Waters Model 600 gradient controller, a Rheodyne (Cotati, CA) Model 7725i sample injector equipped with 20 μl sample loop, a reversed phase (RP) C_{18} analytical column by Phase Sep (25 cm × 4.6 mm ID, 5 μm) and a Water Model 486 tunable absorbance detector controlled by the Millenium (Waters) software. UV detection was performed at 279 nm. The eluent mixture was CH_3CN–H_2O (50:50 v/v), in isocratic mode, at a flow rate of 1 ml/min.

3. Results and discussion

3.1. Characterization of TiO_2 films

The use of sol–gel multistep process led to the production of transparent nanocrystalline TiO_2 thin films with excellent reproducibility, scratch resistance and adherence on the glass substrates. On the contrary, the low cost one step doctor-blade technique produced opaque and thicker films with good uniformity, and with properties closely related to the starting powder material. Scanning electron microscopy was employed to perform at first the surface characterization of the manufactured films. The SEM images, presented in Fig. 1, show that the sol–gel films exhibit a microgranular and flat surface, whereas the doctor-blade films are rougher, forming a sponge like structure. Additionally, cross-section profiles give a thickness of about 5 μm for the Degussa P25 films, while it is demonstrated that the sol–gel films are 500–600 nm thick.

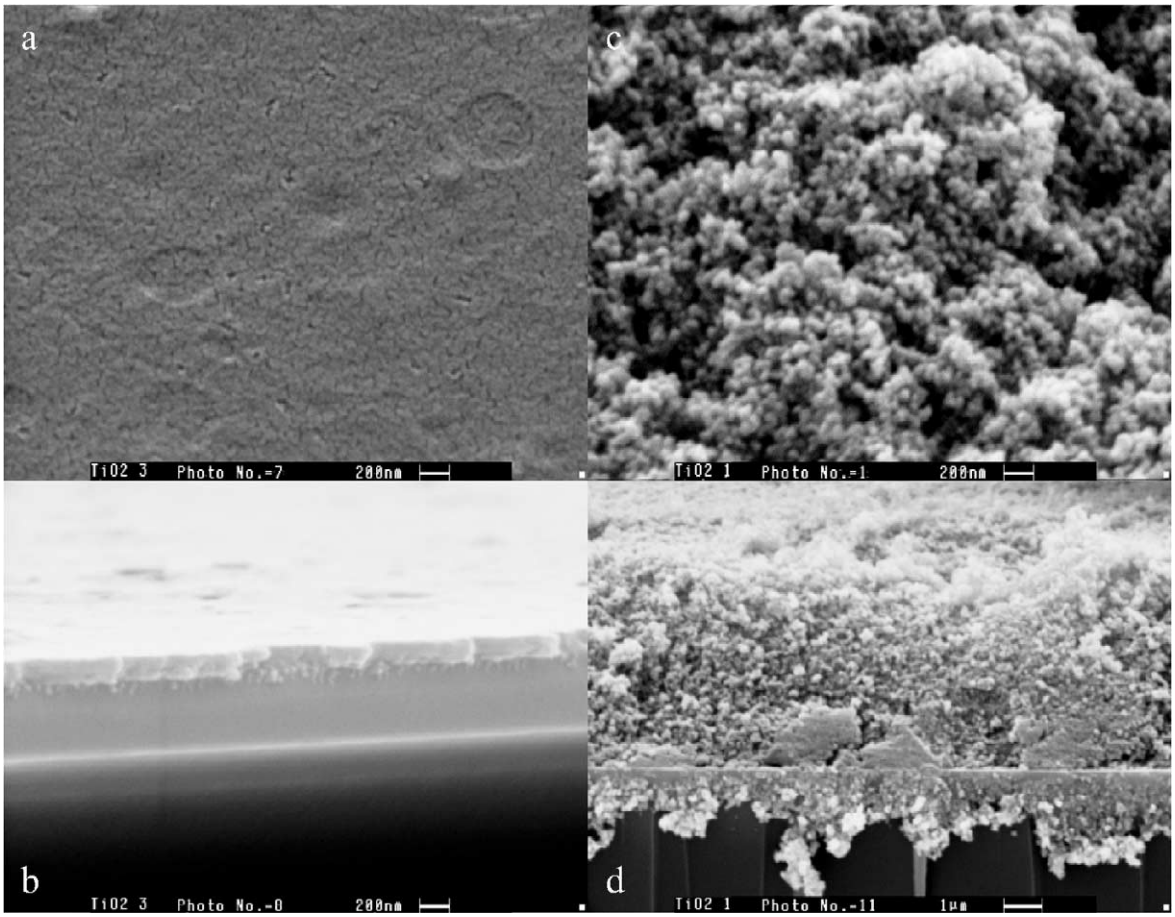

Fig. 1. SEM images of a sol–gel TiO_2 film: (a) top view; (b) cross-section and of a doctor-blade TiO_2 film; (c) top view; (d) cross-section.

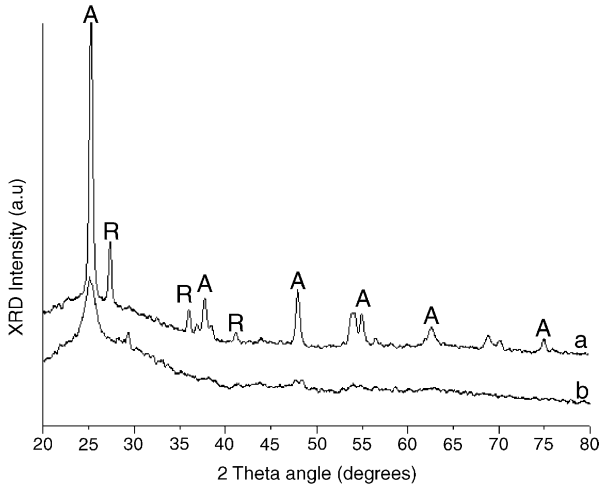

Fig. 2. XRD patterns of doctor-blade (a) and sol–gel (b) TiO_2 films: A, anatase and R, rutile reflections.

The X-ray diffraction patterns, Fig. 2, show that the films prepared by the doctor-blade procedure present very good crystallization. Reflections characteristic of both anatase and rutile TiO_2 phases are easily detected. The presence of the rutile phase can be understood by the fact that the original material, Degussa P25, is a mixture of anatase (70%) and rutile (30%). In the diffraction pattern of the sol–gel TiO_2 films, only a broad peak at 25.116° corresponding to (1 0 1) reflections of the anatase phase of TiO_2 could be identified [23]. It is strongly proposed that such a broad XRD pattern is due to poor crystallization and/or the small size of the TiO_2 particles. Furthermore, crystallite sizes calculated by Scherrer's formula [24] (assuming no crystal distortion in the lattice) were 21 nm for the doctor-blade technique manufactured films and 7 nm for the sol–gel films.

To discriminate the local order characteristics of the TiO_2 films, we applied non-resonant Raman spectroscopy. The technique is non-destructive, capable to elucidate the titania structural complexity as peaks from each crystalline phase are clearly separated in frequency, and therefore the anatase and rutile phases are easily distinguishable [25]. The Raman spectra together with the assigned vibrational modes [6,26] presented in Fig. 3, show that the materials are well crystallized, without overlapped broad peaks and low number of imperfect sites. Vibration peaks at 140, 195, 393, 514, 637 cm^{-1} and 143, 197, 396, 519, 638 cm^{-1} for Degussa P25 and sol–gel samples, respectively, are present in the Raman spectra. These peaks are unambiguously attributed to the anatase modification. Although anatase nanoparticles are the predominant species, however, rutile phase is observed as a broad peak at 446 cm^{-1} for the Degussa P25 sample. The presence of this peak is expected and can be attributed to the initial composition of the TiO_2 powder (∼30:70% rutile/anatase). A special attention must be given to the strong and well-resolved Raman peak observed at 140 cm^{-1} (Eg anatase peak) for the Degussa P25 sample. For the sol–gel sample this peak is more intense and slightly shifted to higher frequencies (143 cm^{-1}), probably due to a smaller size particles [27–29].

3.2. Photodegradation of 3,5-DCP

Photocatalytic experiments took place to evaluate the films as a possible material for water pollutant purification. The photocatalytic activity of the doctor-blade and sol–gel TiO_2 films deposited on microscope glass slides was estimated by degradation of a model compound, namely 3,5-DCP, a characteristic member of the phenol family and rather noxious compound. We first checked the pollutant substrate stability under UV illumination in order to separate the effect of the UV light from the catalytic effect.

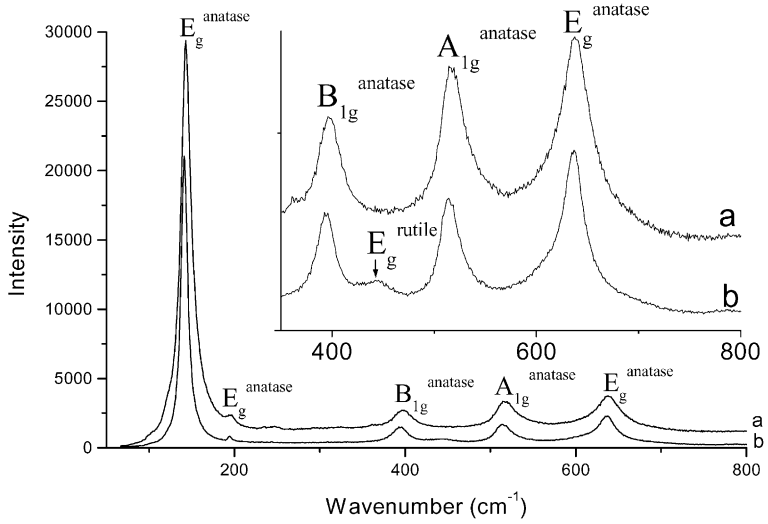

Fig. 3. Raman spectra of doctor-blade (a) and sol–gel (b) TiO_2 films.

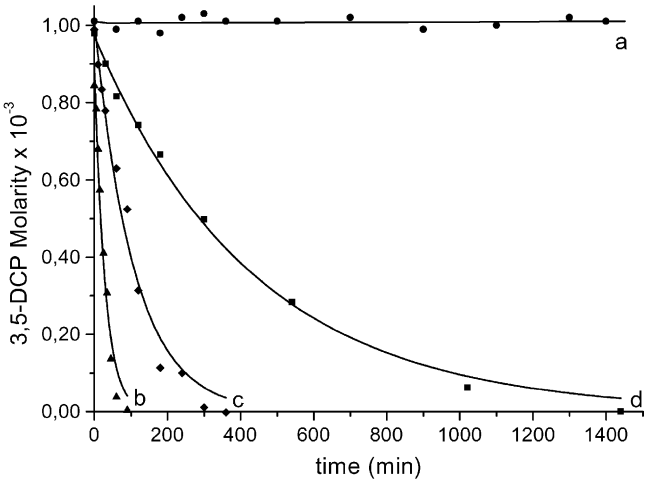

Fig. 4. Decomposition of a 3,5-DCP (10^{-3} M) solution without photocatalyst (a), in the presence of slurry TiO_2 (1625 ppm) solution (b), doctor-blade Degussa P25 TiO_2 immobilized surface (c) and sol–gel TiO_2 films (d).

Thus, an aqueous solution of 3,5-DCP was photolyzed for 6 h without photocatalyst (TiO_2). Fig. 4a reveals that 3,5-DCP remained intact throughout irradiation time. Initial fluctuations in the 3,5-DCP concentration before analysis are due to the physical adsorption of the organic matter on the catalyst surface, during the slurry solution filtration.

The presence of the TiO_2 materials, either in slurry (Fig. 4b), see below, or immobilized on glass surfaces (Fig. 4c and d) results in effective photocatalytic decomposition of the organic pollutant. Analysis of the photolyzed solutions showed the presence of several chlorinated or not organic intermediates and also confirmed the gradual formation of carbon dioxide and chloride anions. To a first approximation the two modes of decomposition (i.e. slurry TiO_2 and TiO_2 films made by doctor-blade technique) seem to proceed through the same intermediates, Fig. 5a and b. This is well understood as both the slurry and the doctor-blade films are composed of the same material (Degussa P25). However, the sol–gel TiO_2 films exhibit minor differences, Fig. 5c, indicating some different intermediate products. This is probably due to the fact that in the sol–gel film only the anatase modification is present.

Under the experimental conditions used, the photocatalytic curves seem to follow first-order reaction kinetics. Initial reaction conditions in Fig. 4 provide realistic comparison of the photodegradation rates. To a reasonable approximation, the slope of the photodegradation profiles corresponds to a relative pseudo-first-order rate constant (min^{-1}). Kinetic parameters, percentage of mineralization after 1 h of illumination and time for complete degradation of 3,5-DCP are summarized in Table 1. The photocatalytic performance of the doctor-blade films (37%) is significantly higher (at least two times) than that of sol–gel films (15%). Complete pollutant degradation with the doctor-blade TiO_2 films was achieved after about 360 min of illumination and for the sol–gel films after about 1600 min, respectively.

Table 1
Photocatalytic efficiency towards 3,5-DCP Degradation (%), average grain diameter, roughness, fractal dimension, for sol–gel and doctor-blade TiO_2 films. Kinetic parameters are also cited

Sample	Doctor-blade technique	Sol–gel technique
Thickness (μm)	5	0.5–0.6
Average grain diameter (nm)		
AFM	20	10
X-ray	21	7
Roughness, Rms (nm)	28.94	0.35
Fractal dimension (D_f)	2.17	2.41
Max of height distribution (nm)	88.4	1.3
Degradation (%) 1 h illumination	36.77	14.84
Time to complete mineralization (min)	360	1600
Rate constant (min^{-1})	0.0079	0.0023

3.3. Surface properties and photocatalytic efficiency

It is obvious that the doctor-blade films are more efficient catalysts, comparing to the sol–gel films. This can be explained on the basis of surface characteristics, such as morphology and film thickness. In order to better understand the differences between doctor-blade and sol–gel films and express this in terms of surface parameters, we have undertaken their characterization by atomic force microscopy. Fig. 6a and b presents $1 \times 1\,\mu m^2$ surface plots (three-dimensional representations) together with top views for both films and surface parameters such as minimum (average) grain diameter, roughness and fractal dimension are given in Table 1. The films consist of interconnected grain particles fused together but it is clear that their morphology and surface characteristics are completely different. In fact, in the case of the doctor-blade films, the average grain diameter is about 20 nm, at least two times higher than that of the sol–gel films (10 nm). Both values are in excellent agreement with the X-ray diffraction results. The particles built up high mountains and deep valleys and their height histogram shows a Gaussian-like distribution with a maximum at 88 nm. On the contrary, the surface of the sol–gel films is more uniform and the size of the surface characteristics is literally lower (the height histogram shows particles with a distribution maximum only just 1.3 nm). These results are in excellent accordance with the roughness analysis. The R_{ms} (=the standard deviation of the Z values, Z being the total height range analyzed) values listed in Table 1 show that the doctor-blade TiO_2 films present surface characteristics of higher size in comparison with sol–gel films.

Looking carefully at the 3D surface plots one can see that the sol–gel films show a more complicated configuration. In order to evaluate and compare the geometric complexity of the film surfaces, qualitative analysis including measurements of parameters such as feature frequency and fractal

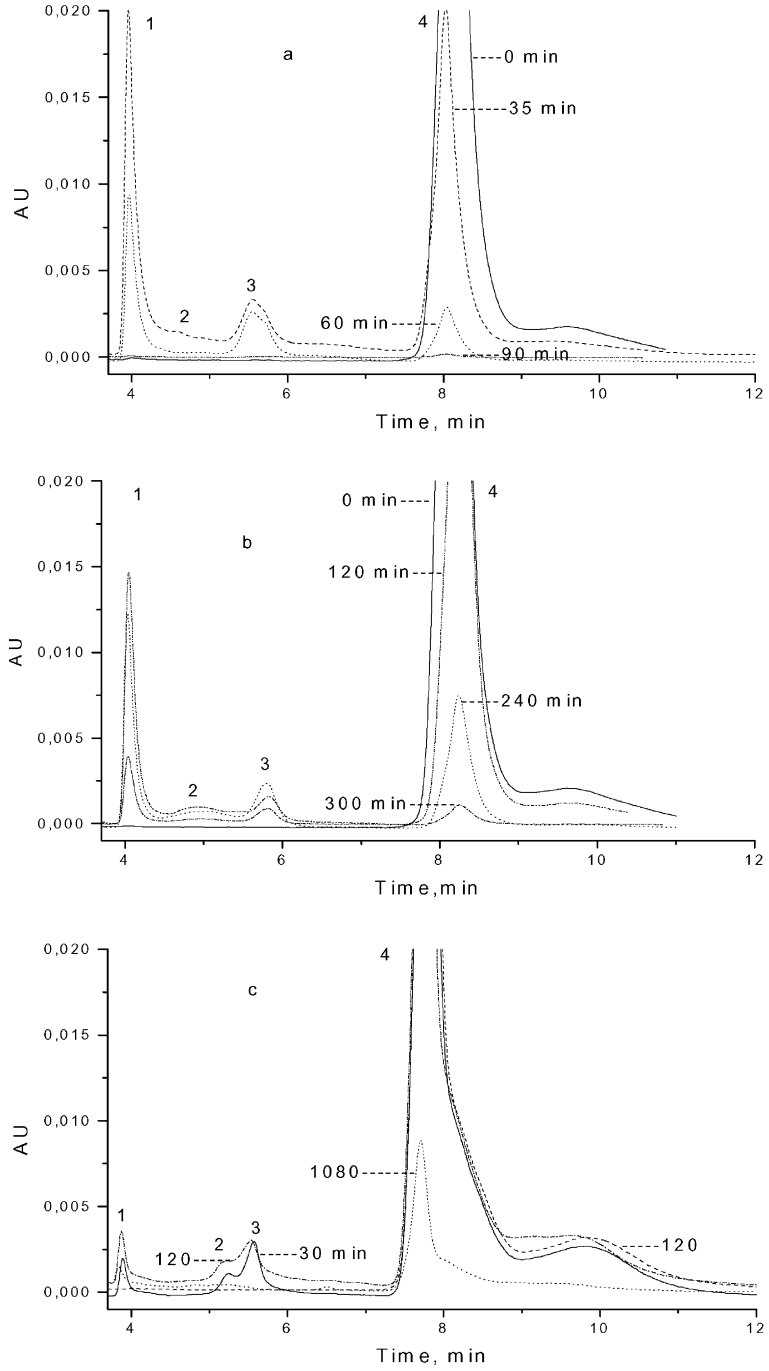

Fig. 5. HPLC–UV chromatograms of photolyzed: (a) TiO_2 slurry; (b) doctor-blade TiO_2 films; (c) sol–gel TiO_2 films of 3,5-DCP (10^{-3} M). Photolysis time is indicated on chromatograms; 1, 2, 3 are intermediate products, 4 is 3,5-DCP.

dimension D_f [17,30–32] (a parameter which reflects the scaling behavior and is an intrinsic property of the material, $3 \geq D_f \geq 2$) was performed. The fractal analysis has shown that the prepared films exhibit also self-affine scaling character over a significant range of length scales as a consequence of a "chaotic" dynamic deposition process, very sensitive to the initial conditions. It is worthwhile mentioning that the sol–gel films have higher fractal dimension D_f than the doctor-blade films (Table 1). The measured values were 2.41 ($\pm$0.02) and 2.17 ($\pm$0.02), respectively. This difference can be explained taking into account the fact that the fractal dimension D_f characterizes mainly the complexity of the surface and not its texture and roughness. The sol–gel TiO_2 films present a more complex topography characterized by a greater number of surface features of higher frequency. The fractal dimension (D_f) parameter influences the

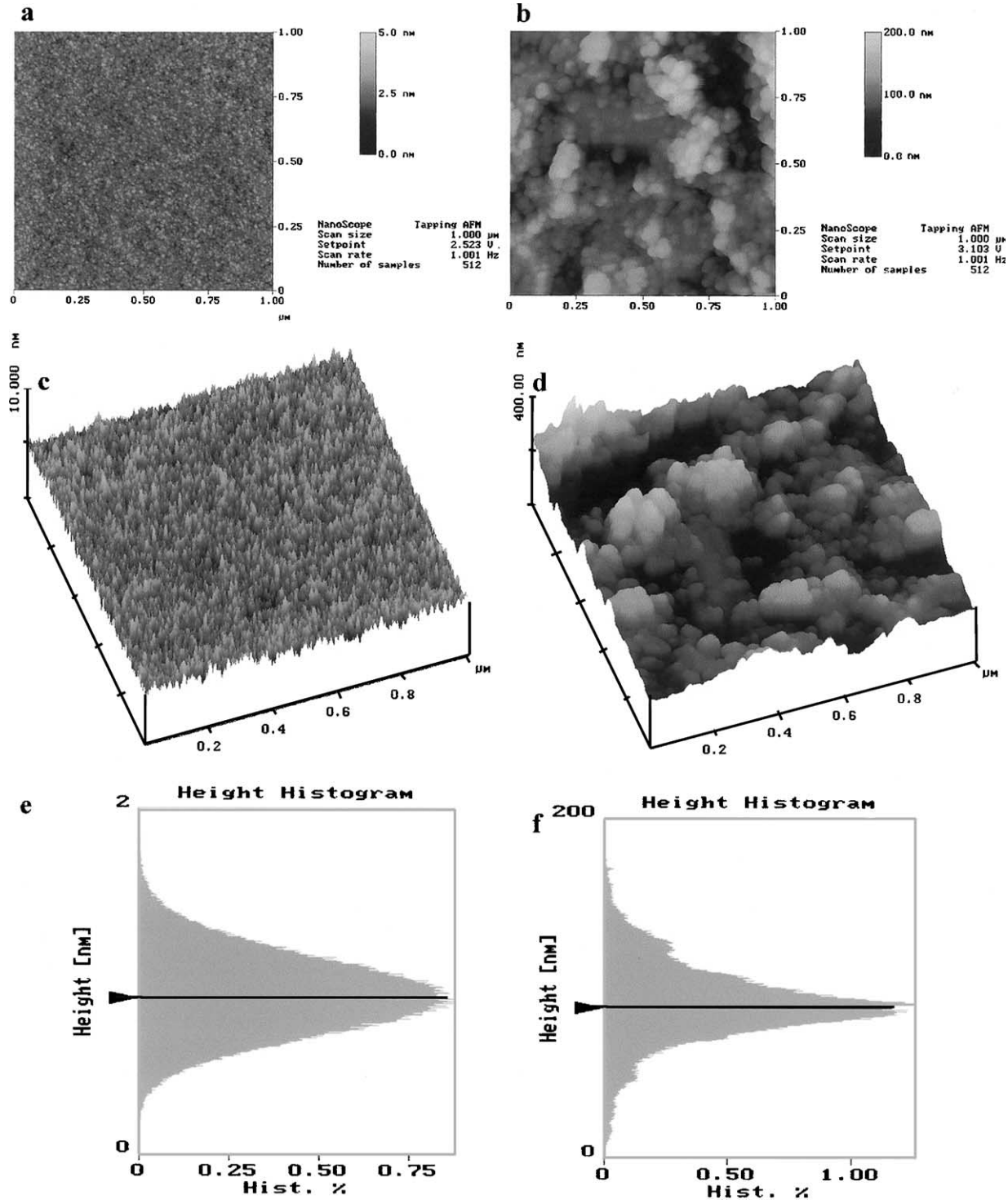

Fig. 6. AFM pictures of a sol–gel TiO_2 film: (a) top view; (b) 3D image; (e) height distribution and of a doctor-blade TiO_2 film; (c) top view; (d) 3D image; (f) height distribution.

effective surface extension *S*. In fact, these parameters are related by the equation

$$S = cR^{D_f}$$

where *c* is a constant that accounts for the finite fluctuations around the 0-level and *R* the linear size of the fractal surface [31]. So, it is clearly evident that the effective surface area in this case is several hundred times greater than the one of a flat *Euclidean* non-fractal surface ($S \sim R^2$). Thus, fractal films show an amazing ability to efficiently capture photons, throughout thick semiconducting network acting in a *sponge*-like way.

However, increasing fractality is not a unique way to achieve the best photocatalytic results. The grain diameter of the TiO_2 nanoparticles is an essential parameter to consider [33]. Taking into account the heterogeneous photocatalytic mechanism of a thin film TiO_2 catalyst, the following steps typically take place [34]: (i) light absorption on the photocatalytic surface (ii) chemical transformation of the molecule while several reaction surface sites are visited (iii) desorption to the liquid phase. Thus, besides the above two parameters (fractal dimension and grain diameter), the height and roughness of surface features must also be considered. As a result, although sol–gel films have a more complex surface structure, their ability to capture the incident photon energy is expressively lower than that of the doctor-blade films. The later present increased roughness resulting from surface characteristics of important height. As a result, the doctor-blade films are endowed with a higher real surface extension, which readily favors the photodecomposition process. In fact, such a surface not only permits the adsorption of a greater number of pollutant molecules, but also creates a rough environment where multiple light reflection can occur, thus considerable increasing the amount of the adsorbed photons.

To evaluate the catalytic strength changes due to immobilization of the catalyst and compare the films efficiency to the Degussa P25 powder, the film weight was measured. The slurry concentration of TiO_2 was then adjusted to meet the exact quantity of TiO_2 Degussa's P25 immobilized film, in order to safely compare the obtained results (it was impossible, however, to organize the same experiments with titania sol–gel films, as the latter demonstrate scratch resistance and excellent adherence). Thus, a pollutant solution (4 ml) was also photolyzed in the presence of a suspension (dispersion) of Degussa P25 powder ($0.0065\,g = 1625\,ppm$) and the results are represented in Fig. 4b. The slope for the slurry is greater than that of the films, showing a considerably higher efficiency as photocatalyst. Complete degradation of 3,5-DCP occurs in less than 100 min. According to kinetic models for photocatalytic degradation of organic contaminants over titania thin film catalysts, the rate of degradation is limited by liquid-film transfer, diffusion, adsorption or a combination of these three factors [35]. It is worth mentioning that on TiO_2 thin film samples, only part of the catalyst is exposed to the pollutant solution and can therefore be photocatalytically active. As a result, a decrease on the overall photocatalytic performance of thin films compared to slurry solution is expected. In fact, one must have in mind that during the thermal treatment of the doctor-blade TiO_2 films no significant change in the structural modification was observed, this difference can be easily understood if one considers that the photocatalytic process is a surface and not a volume or mass phenomenon. The active photocatalyst is the illuminated TiO_2 material, which can be in contact with the organic pollutant, and in the case of the film this only concerns its external surface. As the Degussa's powder surface area is very high ($\sim 50\,m^2/g$), the slurry's surface is much higher than the film's real external surface.

3.4. Repeatability, endurance tests and perspectives

The strength and reproducibility of the photocatalytic activity on the TiO_2 doctor-blade films were examined in order to check their potential use in practical systems. Thus, the same immobilized TiO_2 film surface was used in 10 consecutive photolysis experiments (cycles) of new added pollutant substrate quantities and the results are presented in Fig. 7.

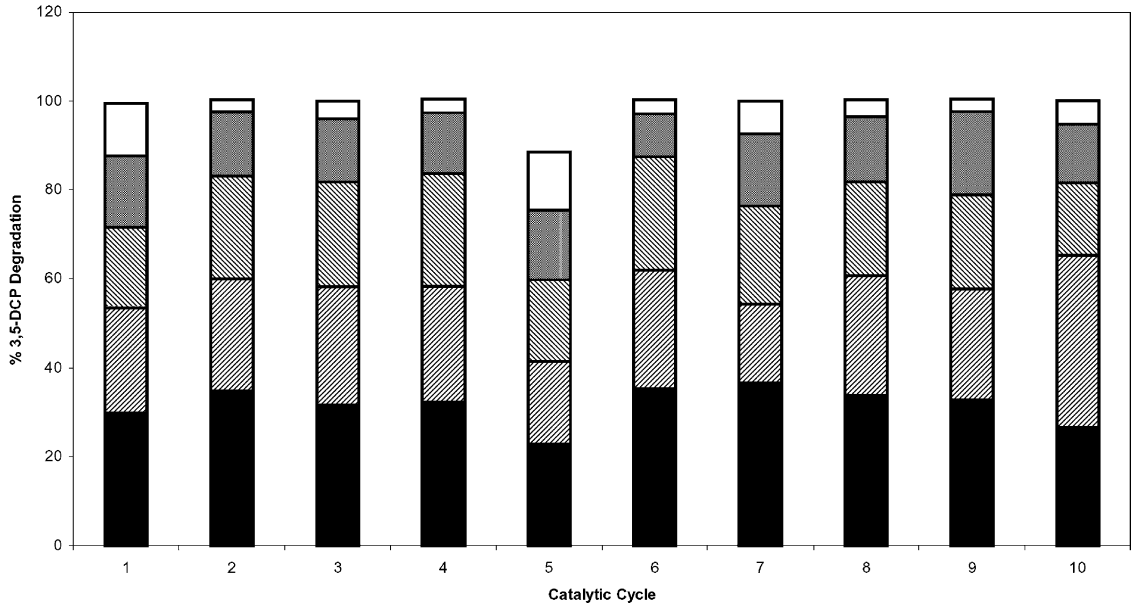

Fig. 7. Reproducibility tests. Decomposition percentage of 3,5-DCP versus time as a function of the cycle number using a doctor-blade TiO_2 thin film catalyst. Each column step corresponds to 60, 120, 180, 240 and 300 min of illumination, respectively.

Each experiment included complete decomposition of the 3,5-DCP and perfectly reproduced the initial results reported in Fig. 4c. On the other hand, several doctor-blade TiO_2 films were continuously tested as photocatalysts for checking the lifetime and stability. The tests covered a four months period during which no sign of activity loss, decrease or time dependence was observed.

The obtained results with the doctor-blade technique make further work on the subject very encouraging. In fact, such a simple, one step and low cost method permits the immobilization of the catalyst as a film and presents the advantage of easier photocatalyst separation. In addition, it opens the possibility to develop more efficient photocatalysts in the form of porous and high surface area inorganic oxide matrixes by using different precursor materials. In this direction, the use of TiO_2 powders with long-range particle size distribution may produce films with very rough surfaces and high efficiency in light captivation. Furthermore, the deposition of these films on a conductive support and the application of an external anodic bias could suppress the recombination between the photogenerated electron–hole pairs and thus considerably increase the efficiency of the photocatalytic degradation [36].

Acknowledgements

We appreciate valuable assistance from Fotini Papadimitriou for obtaining the AFM images. Thanks must be addressed to Delis AE Athens, Greece, and Degussa AG Frankfurt, Germany, for generously providing the TiO_2 Degussa P25 powder. Financial support from NCSR "Demokritos" (Dimoerevna 598 project), Empeirikeion Foundation and General Secretariat for Research and Technology of Greece (EPET II, Greece–France and Greece–Czech Republic bilateral collaboration projects) is also greatly acknowledged.

References

[1] O. Legrini, E. Oliveros, A.M. Braun, Chem. Rev. 93 (1993) 671.
[2] M.R. Hoffmann, S.T. Martin, W. Choi, D.W. Bahnemann, Chem. Rev. 95 (1995) 69.
[3] H. Kuster, J. Ebert, Thin Solid Films 70 (1980) 43.
[4] B. O'Regan, M. Grätzel, Nature 353 (1991) 737.
[5] S. Burnside, S. Winkel, K. Brooks, V. Shklover, M. Grätzel, A. Hinsch, R. Kinderman, C. Bradbury, A. Hagfeldt, H. Pettersson, J. Mater. Sci. 11 (2000) 355.
[6] P. Falaras, A. Hugot-Le Goff, M.C. Bernard, A. Xagas, Sol. Energy Mater. Sol. C 64 (2000) 167.
[7] L. Kavan, D. Fattakhova, P. Krtil, J. Electrochem. Soc. 146 (1999) 1375.
[8] A. Fujishima, K. Hashimoto, T. Watanabe, TiO_2 Photocatalysis, Fundamentals and Applications, Bkc, Inc., Tokyo, 1999.
[9] A. Fujishima, T.N. Rao, D.A. Tryk, J. Photochem. Photobiol. C 1 (2000) 1.
[10] A. Mills, S. Le Hunte, J. Photochem. Photobiol. A 108 (1) (1997) 1.
[11] K. Hashimoto, J. Phys. Chem. B 102 (10) (1998) 1724.
[12] I. Sopyan, M. Watanabe, S. Murasawa, K. Hashimoto, A. Fujishima, J. Photochem. Photobiol. A 98 (1996) 79.
[13] D.F. Ollis, CR Acad. Sci. Ser. IIC 3 (6) (2000) 405.
[14] O.M. Alfano, D. Bahnemann, A.E. Cassano, R. Dillert, R. Goslich, Catal. Today 58 (2000) 199.
[15] M.I. Litter, Appl. Catal. B 23 (1999) 89.
[16] C. Minero, E. Pelizzetti, P. Pichat, M. Sega, M. Vincenti, Environ. Sci. Technol. 29 (9) (1995) 2226.
[17] A.P. Xagas, E. Androulaki, A. Hiskia, P. Falaras, Thin Solid Films 357 (2) (1999) 173.
[18] L.H. Keith, W.A. Telliard, Environ. Sci. Technol. 13 (1979) 416.
[19] M.K. Nazeeruddin, A. Kay, I. Rodicio, R. Humphry-Baker, E. Müller, P. Liska, N. Vlachopoulos, M. Grätzel, J. Am. Chem. Soc. 115 (1993) 6382.
[20] K. Kalyanasundaram, M. Gratzel, Coord. Chem. Rev. 77 (1998) 347.
[21] V. Shklover, M.-K. Nazeeruddin, S.M. Zakeeruddin, C. Barbe, A. Kay, T. Haibach, Steurer, R. Hermann, H.-U. Nissen, M. Gratzel, Chem. Mater. 9 (1997) 430.
[22] E. Scolan, C. Sanchez, Chem. Mater. 10 (1998) 3217.
[23] JCPDS Powder Diffraction File, Card 21-1272, JCPDS, International Centre for Diffraction Data, Swarthmore, PA, 1980.
[24] H.P. Klug, L.E. Alexander, X-ray Diffraction Procedures, Wiley, New York, 1954 (Chapter 9).
[25] V.V. Yakovlev, G. Scarel, C.R. Aita, S. Mochizuki, Appl. Phys. Lett. 76 (2000) 1107.
[26] A. Turkovic, M. Ivanda, A. Drasner, Thin Solid Films 198 (1991) 199.
[27] W. Ma, Z. Lu, M. Zhang, Appl. Phys. A 66 (1998) 621.
[28] A. Gajović, M. Stubičar, M. Ivanda, K. Furić, J. Mol. Struct. 563–564 (2001) 315.
[29] S. Musić, M. Gotić, M. Ivanda, A. Sekulić, K. Furić, A. Turković, S. Popović, Mater. Lett. 28 (1996) 225.
[30] B. Mandelbrot, The Fractal Geometry of Nature, Freeman, New York, 1982.
[31] A. Provata, P. Falaras, A. Xagas, Chem. Phys. Lett. 297 (5–6) (1998) 484.
[32] P. Falaras, Sol. Energy Mater. Sol. Cells 53 (1998) 163.
[33] N. Serpone, D. Lawless, R. Khairutdinov, E. Pelizzetti, J. Phys. Chem. 99 (1995) 16655.
[34] N. Serpone, A. Salinaro, A. Emeline, V. Ryabchuk, J. Photochem. Photobiol. A 130 (2000) 83.
[35] H.T. Chang, N.M. Wu, F. Zhu, Wat. Res. 34 (2000) 407.
[36] J.M. Kesselman, O. Weres, N.S. Lewis, M.R. Hofmann, J. Phys. Chem. B 101 (1997) 2637.